

ENVIRONMENTAL RESEARCH
LETTERS

LETTER


Response of moist and dry processes in atmospheric blocking to climate change

OPEN ACCESS

RECEIVED
28 April 2022REVISED
9 July 2022ACCEPTED FOR PUBLICATION
15 July 2022PUBLISHED
27 July 2022

Original Content from
this work may be used
under the terms of the
[Creative Commons
Attribution 4.0 licence](#).

Any further distribution
of this work must
maintain attribution to
the author(s) and the title
of the work, journal
citation and DOI.

Daniel Steinfeld^{1,2,*} , Michael Sprenger², Urs Beyerle² and Stephan Pfahl³¹ Institute of Geography and Oeschger Centre for Climate Change Research, University of Bern, Bern, Switzerland² Institute for Atmospheric and Climate Science, ETH Zürich, Zürich, Switzerland³ Institute of Meteorology, Freie Universität Berlin, Berlin, Germany

* Author to whom any correspondence should be addressed.

E-mail: daniel.steinfeld@giub.unibe.ch**Keywords:** atmospheric blocking, latent heating, moist and dry processes, air parcel trajectories, climate change, extreme weather, ensemble climate simulations**Abstract**

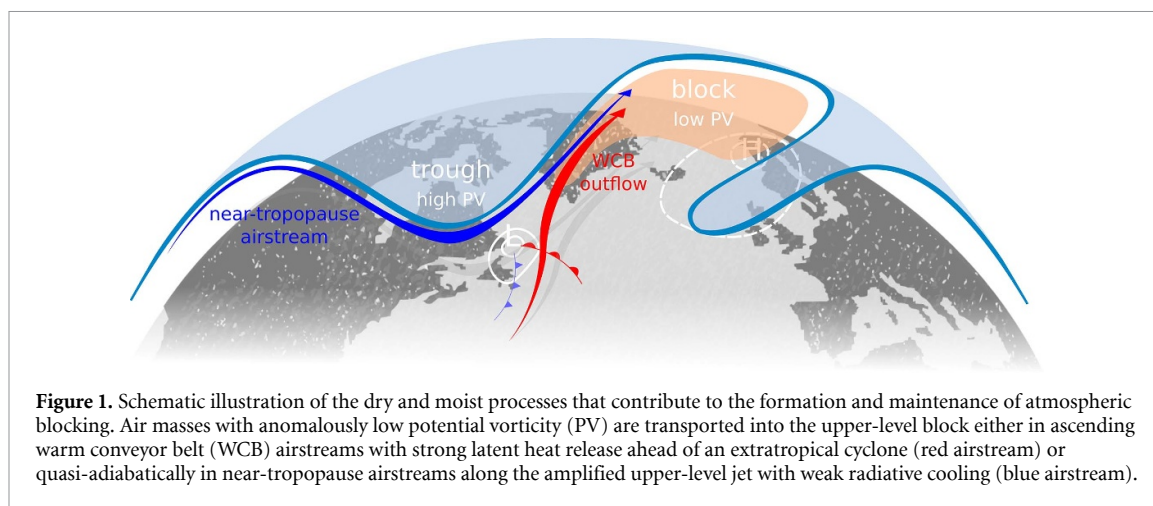
Weather extremes are often associated with atmospheric blocking, but how the underlying physical processes leading to blocking respond to climate change is not yet fully understood. Here we track blocks as upper-level negative potential vorticity (PV) anomalies and apply a Lagrangian analysis to 100 years of present-day (~2000) and future (~2100, under the RCP8.5 scenario) climate simulations restarted from the Community Earth System Model–Large Ensemble Project runs (CESM-LENS) to identify different physical processes and quantify how their relative importance changes in a warmer and more humid climate. The trajectories reveal two contrasting airstreams that both contribute to the formation and maintenance of blocking: latent heating in strongly ascending airstreams (moist processes) and quasi-adiabatic flow near the tropopause with weak radiative cooling (dry processes). Both are reproduced remarkably well when compared against ERA-Interim reanalysis, and their relative importance varies regionally and seasonally. The response of blocks to climate change is complex and differs regionally, with a general increase in the importance of moist processes due to stronger latent heating (+1 K in the median over the Northern Hemisphere) and a larger fraction (+15%) of strongly heated warm conveyor belt air masses, most pronounced over the storm tracks. Future blocks become larger (+7%) and their negative PV anomaly slightly intensifies (+0.8%). Using a Theil–Sen regression model, we propose that the increase in size and intensity is related to the increase in latent heating, resulting in stronger cross-isentropic transport of air with low PV into the blocking anticyclones. Our findings provide evidence that moist processes become more important for the large-scale atmospheric circulation in the midlatitudes, with the potential for larger and more intense blocks.

1. Introduction

Atmospheric blocking describes the formation of persistent and quasi-stationary anticyclonic circulation anomalies that disrupt the large-scale westerly flow and eastward progression of synoptic weather systems (Berggren *et al* 1949, Rex 1950). Blocks are often associated with and contribute to extreme weather such as heatwaves (Pfahl and Wernli 2012, Wehrli *et al* 2019), cold spells (Buehler *et al* 2011, Sillmann *et al* 2011, Brunner *et al* 2017), heavy precipitation (Lenggenhager and Martius 2020) and compound events (Kautz *et al* 2022). As a result,

there is considerable interest in understanding how the occurrence of blocks and their contribution to extreme surface weather might change as the climate warms (Sillmann and Croci-Maspoli 2009, Brunner *et al* 2018, Schaller *et al* 2018, Woollings *et al* 2018, Nabizadeh *et al* 2021).

The influence of climate change on blocking remains an open question (Hoskins and Woollings 2015, Woollings *et al* 2018). Climate models still struggle in representing present-day blocking statistics and generally underestimate blocking frequency, particularly over the North Atlantic (e.g. Davini and D'Andrea 2016, 2020, Woollings *et al* 2018,



Schiemann *et al* 2020), which introduces uncertainty in future projections (Hassanzadeh *et al* 2014). Enhanced warming in near-surface polar regions (denoted as polar amplification, Serreze and Barry 2011) and in the tropical upper troposphere (Yin 2005) have competing effects on the midlatitude large-scale circulation, storm tracks and the propagation of synoptic Rossby waves (e.g. Barnes and Screen 2015, Harvey *et al* 2015, Shaw *et al* 2016), which are intimately linked to the development of atmospheric blocking (Altenhoff *et al* 2008, Nakamura and Huang 2018). Furthermore, projected increases in atmospheric moisture content (Held and Soden 2006, Schneider *et al* 2010) and associated increases in latent heat release (Pfahl *et al* 2015) and static stability (O’Gorman and Schneider 2008) have significant ramifications on midlatitude weather systems and the large-scale circulation. Future changes in blocking are complex and not well understood, but are likely to be small compared to internal variability (Deser *et al* 2012, Barnes *et al* 2014, Blackport and Screen 2020), and climate model ensemble projections indicate a weak reduction or weak spatial shift in blocking occurrence (e.g. Dunn-Sigouin and Son 2013, Masato *et al* 2013, Davini and D’Andrea 2020), depending on the model and blocking index used (Woollings *et al* 2018). Recent studies have further investigated the effects of climate change on blocking properties, such as duration (Huguenin *et al* 2020), propagation (Riboldi *et al* 2020) and the size and 3D structure (Nabizadeh *et al* 2019, 2021). They showed that duration and propagation are projected to remain fairly constant, while blocks are expected to become larger. The underlying physical processes that may cause such changes have not yet been fully elucidated.

The challenge in predicting the future response of blocking arises from the multiple, competing processes involved in blocking formation and maintenance, and the importance of processes can vary for different regions (Nakamura *et al* 1997, Drouard and Woollings 2018, Steinfeld and Pfahl 2019,

Drouard *et al* 2021, Miller and Wang 2022). Blocks form when an extended air mass with low potential vorticity (PV) is advected poleward, related to synoptic eddies and a meridionally amplified flow (Colucci 1985, Nakamura and Huang 2018), setting up a large-scale anticyclonic PV anomaly in the upper troposphere beneath an elevated tropopause (Hoskins *et al* 1985). Air masses with low PV are transported into the upper-level block either (a) in ascending warm conveyor belt (WCB) airstreams with strong latent heat release (moist processes, see Pfahl *et al* 2015, Steinfeld and Pfahl 2019), or (b) quasi-adiabatically in near-tropopause airstreams along the amplified upper-level jet (dry processes, e.g. Shutts 1983, Yamazaki and Itoh 2013, Luo *et al* 2014), as illustrated schematically in figure 1. As for moist processes, numerical sensitivity experiments demonstrated that blocks with a strong contribution from latent heating are larger and more intense than their dry (without latent heating) counterparts (Steinfeld *et al* 2020), and Nabizadeh *et al* (2021) suggested that latent heating upstream of the block becomes more important in the future. Given the key role of both dry and moist processes in blocking, and the expected increase in moisture content in a warming atmosphere, the question arises how physical processes in blocking respond to climate change.

In this letter, we quantify the relative importance of dry and moist processes throughout the blocking lifecycle, and analyse how these processes and their importance will change in a future, warmer climate. We apply a blocking tracking and Lagrangian trajectory-based diagnostic to 100 years of present-day and future climate ensemble simulations. In this context, we ask three questions: (a) How well are the aforementioned physical processes that lead to the formation of blocks represented in the climate simulations? (b) How does their relative importance change in a warming climate, and are there seasonal and regional differences? and (c) How will future warming change the intensity and size of blocks?

2. Data and methods

2.1. Data

To quantify future changes in the presence of internal variability, we use the output from ten ensemble simulations performed with the NCAR CESM1 model, which incorporates the CAM5 Atmospheric Model (Hurrell *et al* 2013), for two time slices, 1991–2000 for present-day climate (HIST) and 2091–2100 for future climate (RCP8.5). The Community Earth System Model–Large Ensemble Project (CESM-LENS) simulations used in this study were restarted from the first ten members of the CESM-LENS runs (Kay *et al* 2015) in the year 1980 and 2081 to obtain more comprehensive 6 hourly output fields, such as vertical velocity on model levels. The 6 hourly outputs are stored at 1° resolution on 30 vertical hybrid sigma-pressure levels. Historical forcing was applied from 1991 to 2000 and the high-emission Representative Concentration Pathway 8.5 forcing was used for future projections from 2091 to 2100. This provides us with 100 years of simulations for each climate. We obtain projected changes by subtracting the present-day simulations (HIST) from the projected future simulations (RCP8.5).

As a reference data set, we use the 6 hourly ERA-Interim reanalysis (ERA-I) product for the time period 1979–2018 with a spatial resolution of 1° and 60 vertical levels (Dee *et al* 2011). The blocking and trajectory climatology of ERA-Interim is described in Steinfeld and Pfahl (2019).

Only the Northern Hemisphere is considered in this letter. We analyse blocks in all seasons, but highlight seasonal differences between winter (DJF) and summer (JJA).

2.2. Atmospheric blocking

Atmospheric blocks are identified and tracked as negative PV anomalies in the upper-level flow (vertically averaged between 150–500 hPa). We use the blocking index of Schwierz *et al* (2004), with an intensity exceeding -1.3 pvu (PV unit) and 70% contour overlap between consecutive 6 hourly time steps for at least 5 days (for more details, see Croci-Maspoli *et al* 2007, Steinfeld and Pfahl 2019). PV anomalies are determined by subtracting a climatological monthly mean for each corresponding climate and temporally smoothed with a two day running mean filter to remove higher frequency components. We define the blocking size as the spatial extent of the blocking region and blocking intensity as the area-averaged upper-level negative PV anomaly. The advantage of the PV-based index is that it captures the core of the anticyclonic anomaly, allowing us to directly investigate the origin of these air masses and the associated physical processes. We analyse a total of 5900 blocks in HIST, 5500 blocks in RCP8.5 and 2600 blocks in ERA-I.

CESM has been studied in great detail with respect to blocking occurrence and jet stream variability in previous studies (e.g. Kwon *et al* 2018). Like most CMIP5 models, CESM-LENS shows the well-described underestimation of the occurrence of blocking and an overly strong eddy-driven jet in winter, particularly over the North Atlantic (Woollings *et al* 2018, Davini and D'Andrea 2020), but performs reasonably well compared to other CMIP5 models (Huguenin *et al* 2020).

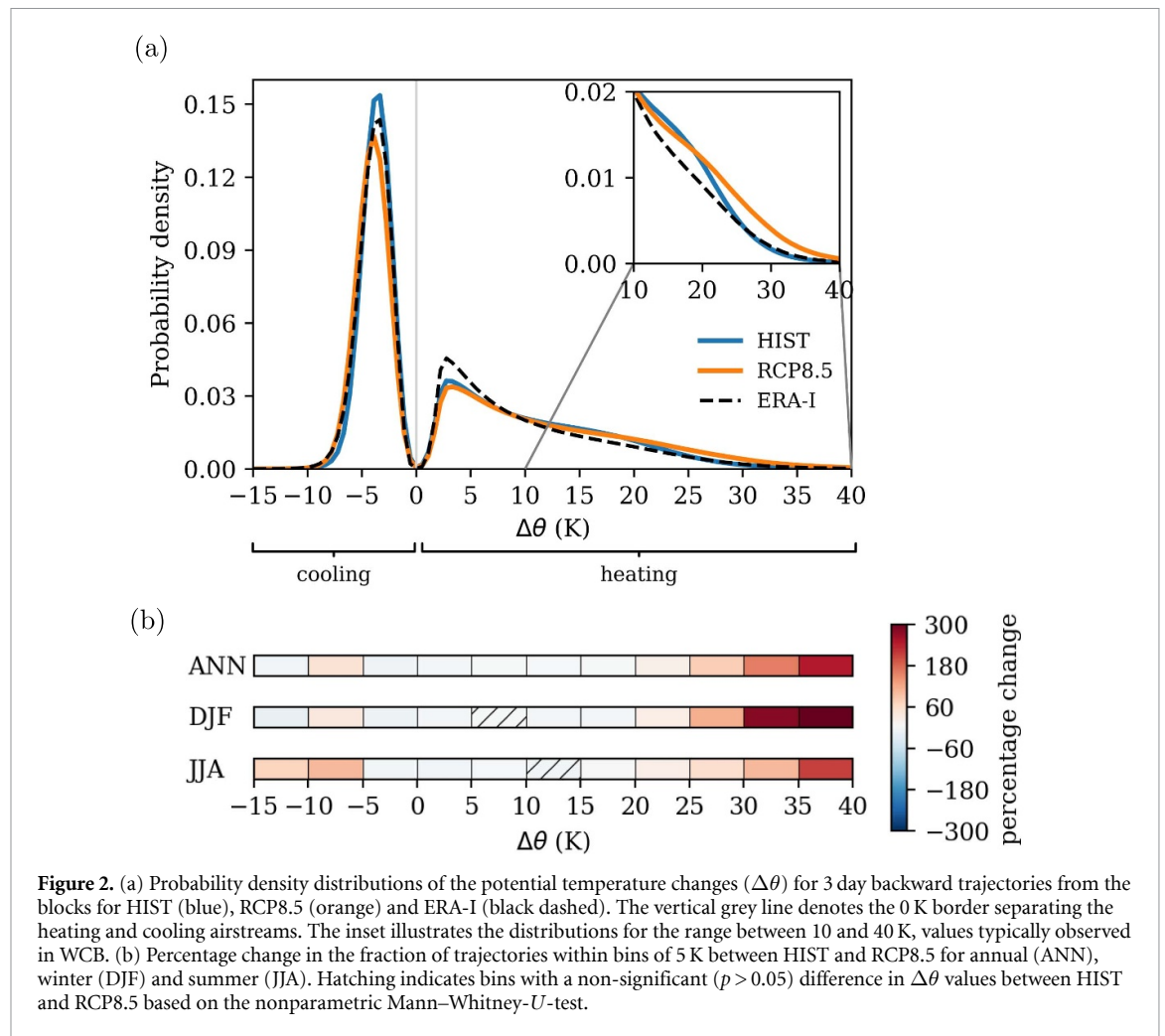
2.3. Trajectory calculation to quantify physical processes

Lagrangian analysis of blocking air masses allows us to identify and quantify the relative importance of different physical processes that govern the formation and maintenance of blocks (e.g. Pfahl *et al* 2015). We use the Lagrangian analysis tool 'LAGRANTO' (Wernli and Davies 1997, Sprenger and Wernli 2015) to calculate kinematic 3 day backward trajectories initiated inside the blocking region every 80 km and vertically every 50 hPa between 500 and 150 hPa. We exclude points located in the stratosphere by selecting air masses with a PV value smaller than 1 pvu. Horizontal position, pressure, moisture content, potential temperature and PV are traced along the trajectories. The origin of the low PV within the block can be attributed to either adiabatic advection or cross-isentropic transport (Croci-Maspoli and Davies 2009). Therefore, we calculate the maximum change in potential temperature ($\Delta\theta$) along each backward trajectory following the procedure of Steinfeld and Pfahl (2019). We will show that trajectories with positive $\Delta\theta$ experience cross-isentropic ascent primarily associated with latent heating during cloud formation (moist processes), and trajectories with negative $\Delta\theta$ experience radiative cooling and quasi-adiabatic advection (dry processes). This characterization by the sign of $\Delta\theta$ will be useful to identify two categories of airstreams with strongly different properties, both contributing to the block's negative PV anomalies (see again figure 1).

3. Results and discussion

3.1. Representation of physical processes in present-day blocking

In order to classify the relative importance of different physical processes that contribute to the block's negative PV anomalies, figure 2(a) shows statistical distributions of $\Delta\theta$ for HIST (blue, across all ten members), RCP8.5 (orange, across all ten members), and ERA-I (dashed black) for all trajectories during the entire blocking lifecycle (onset, maturity, and decay). As known from Steinfeld and Pfahl (2019), $\Delta\theta$ reveals a bimodal distribution with two contrasting airstreams that can be associated with blocking: a cooling airstream ($\Delta\theta < 0$ K) with a Gaussian normal



distribution, and a skewed heating airstream ($\Delta\theta > 0$ K) with a wide range of values up to 40 K. The distributions of $\Delta\theta$ look very similar for ERA-I and CESM-LENS and confirm the main features known from previous studies. For HIST (blue curve), about 47.2% of the trajectories belong to the heating airstream, and consequently, 52.8% to the cooling airstream. These high fractions demonstrate the overall importance of latent heating for atmospheric blocking (see again Pfahl *et al* 2015, Steinfeld and Pfahl 2019). The trajectories of the heating airstream are governed by moist processes. They exhibit strong heating of 9.6 K in the median, and the concurrent loss of specific humidity of -2.9 g kg^{-1} and ascent of around -282 hPa in the 3 days (see table 1) indicate that latent heat release during cloud formation is the dominant physical process. The trajectories in the cooling airstream are radiatively cooled by -3.7 K in the median and governed by dry (quasi-adiabatic) advection with the upper-level westerlies. They are initially dry, and stay approximately on the same pressure level ($\Delta p = -1 \text{ hPa}$) in the 3 days before arriving in the upper-level blocks. 23% of all blocking trajectories (and 48% of the heating trajectories) experience intense heating of more than 10 K in 3 days, which

corresponds to values typically observed in WCB (see Madonna *et al* 2014). WCBs are moist airstreams that ascend rapidly from the midlatitude cyclone's warm sector to the upper troposphere with strong latent heat release. Overall, latent heating is a more intense and rapid process compared to cooling. The trajectories of the heating airstream, in particular WCBs, typically reach higher altitudes and generate stronger negative PV anomalies within the blocking region compared to the cooling airstream (see table 1).

CESM-LENS exhibits biases in the representation of blocks (Kwon *et al* 2018, Athanasiadis *et al* 2020). Therefore, we compare the $\Delta\theta$ distribution of CESM-LENS HIST with ERA-I reanalysis data more closely (figure 2(a) and table 1). HIST reproduces the distribution and fraction of heating and cooling airstreams remarkably well. There is a slight underestimation of weaker heating between 2 and 10 K, which is compensated by an overestimation of stronger heating between 10 and 25 K. Consequently, HIST slightly overestimates the intensity of the median heating by about $+1.3 \text{ K}$, but agrees with ERA-I on the wide range of positive $\Delta\theta$ values in the heating airstream. Despite weaker heating and ascent in ERA-I, the heating airstream in

Table 1. Fraction of blocking trajectories (%) belonging to the cooling ($\Delta\theta < 0$ K) and heating airstream ($\Delta\theta > 0$ K), ensemble-median of maximum potential temperature change ($\Delta\theta$, in K), pressure change (Δp , in hPa) and moisture change (Δq , in g kg^{-1}) in the 3 days before arriving in the block, and PV anomaly inside the block at $t = 0$ (PV' , in pvu). These values are calculated along 3 day trajectories throughout the entire blocking lifecycle.

	Cooling					Heating				
	%	$\Delta\theta$	Δp	Δq	PV'	%	$\Delta\theta$	Δp	Δq	PV'
HIST	52.8	-3.7	-1	-0.1	-0.95	47.2	9.6	-282	-2.9	-1.27
RCP8.5	50.7	-4.0	6	-0.1	-0.84	49.3	10.6	-260	-3.1	-1.29
ERA-I	52.8	-3.8	-1	0	-1.22	47.2	8.3	-232	-2	-1.43

ERA-I produces more intense negative PV anomalies than in HIST. The biases in the cooling airstream are smaller (0.1 K in the median). These differences are probably related to the lower vertical resolution of CESM-LENS with 30 levels compared to ERA-I with 60 levels. Overall, physical processes in blocks are well simulated in CESM-LENS, which was also observed in Nabizadeh *et al* (2021). Therefore, we are confident in drawing inferences about future changes in these physical processes based on CESM projections.

3.2. Future changes in physical processes

Projected future changes (see again figure 2 and table 1) are relatively small, but show that the overall fraction of the heating airstream increases by 2%, while the median $\Delta\theta$ increases by +1 K. A positive shift within the heating airstream from moderate towards more intense latent heating is projected, and consistent with this, an increase in the fraction of WCB trajectories (with more than 10 K heating) by +15%. The fraction of trajectories with $\Delta\theta > 20$ K increases by +56%, and this increase is even stronger for very large $\Delta\theta$ values, especially in winter (see figure 2(b)). The median changes in the cooling airstream are smaller with -0.3 K. While both types of processes are projected to increase in magnitude, this increase is more pronounced for the heating, and moist processes thus become even more active and important in the projected future climate. The hemispheric-wide changes in median $\Delta\theta$ by season (not shown) indicates that the largest (and most robust) increase occurs in winter (+1.1 K), while the increase in summer amounts to +0.6 K. This enhanced latent heating in ascending airstreams can be expected because of the increasing moisture content in a warming atmosphere following the Clausius–Clapeyron relationship (Trenberth 1999, Held and Soden 2006). A similar increase in latent heating and associated PV modification, i.e. stronger PV production in the lower troposphere in extratropical cyclones and persistent anomalies, was found in CESM-LENS future projections (Dolores-Tesillos *et al* 2022) and in idealized climate change simulations (Tamarin and Kaspi 2016, Büeler and Pfahl 2019, Tierney *et al* 2021).

3.3. Spatial and seasonal distribution

Our results so far reveal an overall increased importance of latent heating and a larger contribution of WCBs in future blocks. To further assess how blocks dynamically change in different regions and seasons, we show present-day (HIST) spatial distributions of $\Delta\theta$ and their future changes for winter and summer in figure 3.

Figure 3(a) for winter and figure 3(b) for summer illustrate a large spatial and temporal variability of physical processes in blocking in HIST. From Steinfeld and Pfahl (2019) for ERA-I we know that there are distinct regions where blocks are generally more affected by heating (mean positive $\Delta\theta$) or cooling (mean negative $\Delta\theta$). HIST confirms that heating dominates in blocks over the oceans, in the storm track regions of the North Pacific and North Atlantic, throughout the year. Continental blocks exhibit strong seasonality: heating dominates over the northern Asian continent in summer, while cooling dominates in Ural blocks in winter, European blocks in summer, and high-latitude blocks over the Arctic. We assume that soil moisture availability plays an important role in this seasonality over land (e.g. Fischer *et al* 2007), which is not explored further here. In most regions, the magnitude of heating is much stronger than cooling, reaching mean $\Delta\theta$ values of up to 8 K over the oceans in both seasons. These regions of intense latent heating coincide with the main blocking regions over the oceans (black contours in figure 3(a) and (b)).

Projected future changes (RCP8.5–HIST) in mean $\Delta\theta$ for winter and summer are shown in figures 3(c) and (d). In winter, $\Delta\theta$ increases over large parts of the NH. This increase is larger than +2 K and consistent between the ensemble members over parts of the North Pacific, North Atlantic, North America and Europe. In contrast to this general increase, a decrease in $\Delta\theta$ occurs over the Asian continent and parts of the higher latitudes, mostly in regions where mean $\Delta\theta$ is already negative in HIST (figure 3(a)). However, the decrease has a weaker magnitude of about -0.5 K and the ensemble members mostly disagree on the sign of changes. In summer, $\Delta\theta$ is again projected to increase strongly over the North Pacific and North Atlantic, while $\Delta\theta$ decreases over land

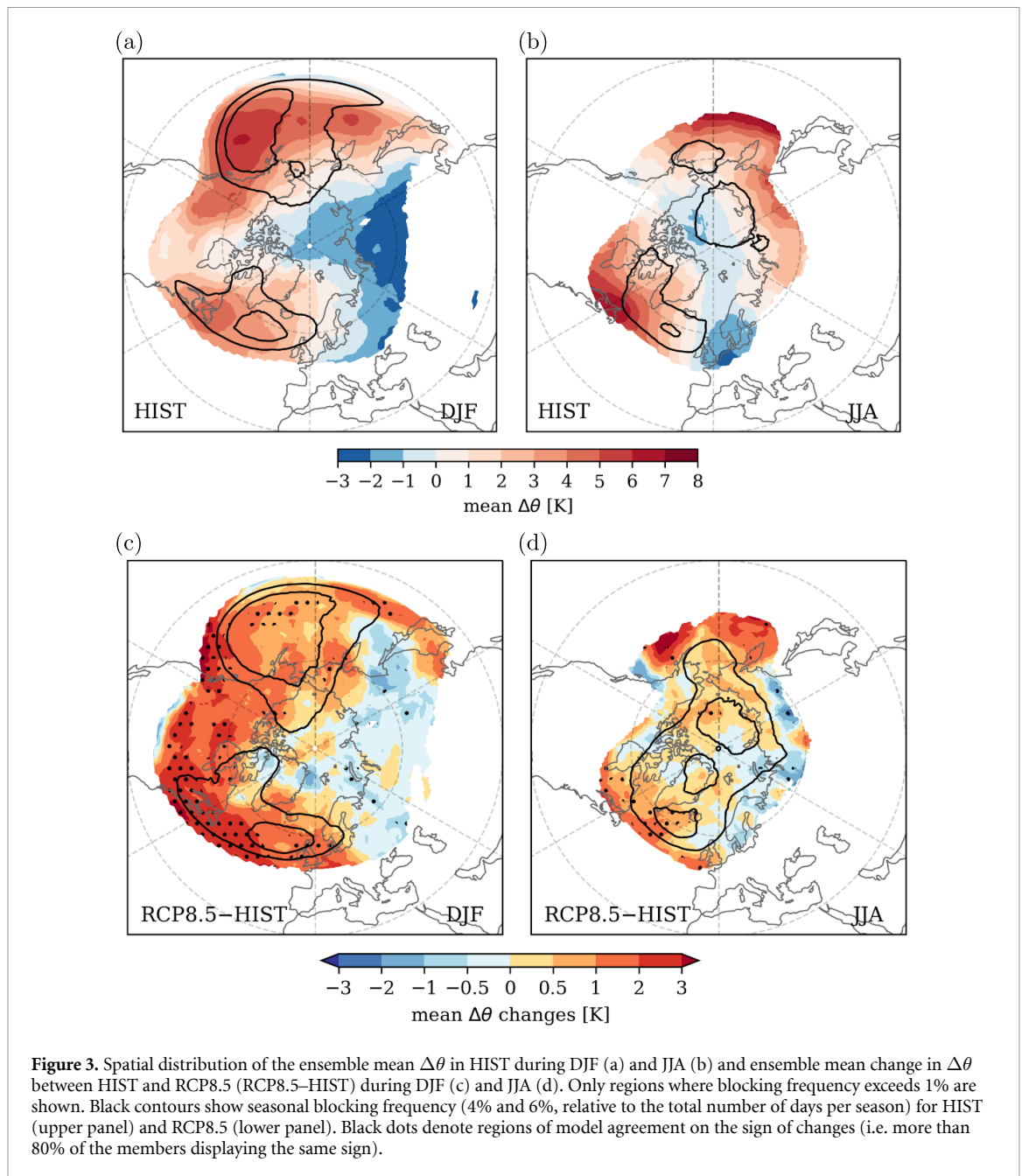


Figure 3. Spatial distribution of the ensemble mean $\Delta\theta$ in HIST during DJF (a) and JJA (b) and ensemble mean change in $\Delta\theta$ between HIST and RCP8.5 (RCP8.5-HIST) during DJF (c) and JJA (d). Only regions where blocking frequency exceeds 1% are shown. Black contours show seasonal blocking frequency (4% and 6%, relative to the total number of days per season) for HIST (upper panel) and RCP8.5 (lower panel). Black dots denote regions of model agreement on the sign of changes (i.e. more than 80% of the members displaying the same sign).

and in parts of the higher latitudes. The agreement between the ensemble members is weaker during summer, but a robust increase in $\Delta\theta$ is projected over the North Atlantic. Regions with a positive $\Delta\theta$ coincide with the main blocking regions in RCP8.5, which are projected to shift eastward in winter and poleward in summer.

The decomposition into cooling and warming trajectories allows us to directly assess their contributions to the projected regional changes. For example, while both types of processes are projected to intensify, it is mainly the latent heating that intensifies strongly in the main blocking regions over the oceans, while cooling intensifies primarily over land. These are the distinct regions where heating and cooling already dominate in the present-day climate (see

again figures 3(a) and (b)). The strongest increase in latent heating in the oceanic storm tracks is consistent with Li *et al* (2014), Yettella and Kay (2017), who found an increase in cyclone-associated precipitation primarily due to increased moisture availability in a warming atmosphere. Because these regions also coincide with the main regions where blocks intensify (Steinfeld and Pfahl 2019), latent heating will become even more important for the onset and re-intensification ('maintenance') of blocks (see next section).

There are regional exceptions to these general findings. Over Europe, for example, latent heating will replace cooling as the dominant process for winter blocks. On the other hand, a reduced contribution of latent heating is projected for summer blocks

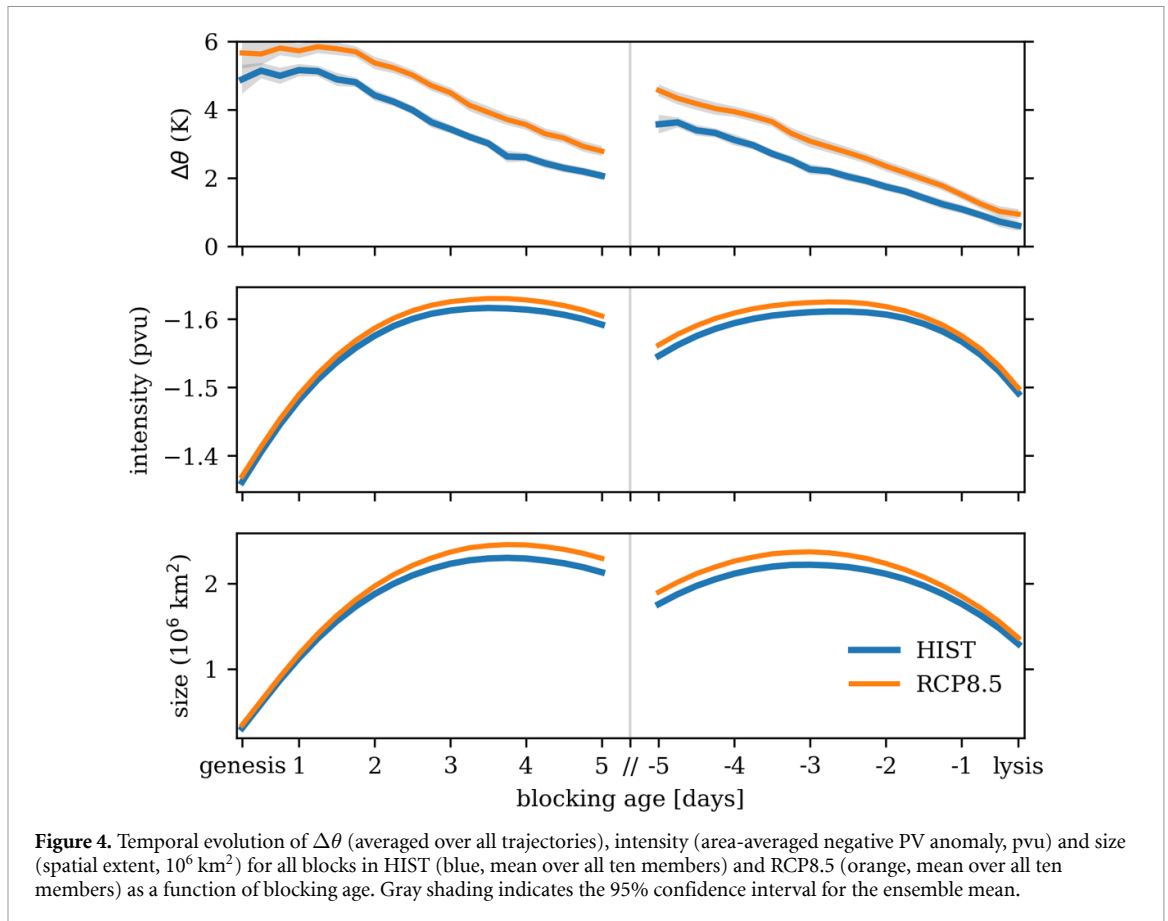


Figure 4. Temporal evolution of $\Delta\theta$ (averaged over all trajectories), intensity (area-averaged negative PV anomaly, pvu) and size (spatial extent, 10^6 km²) for all blocks in HIST (blue, mean over all ten members) and RCP8.5 (orange, mean over all ten members) as a function of blocking age. Gray shading indicates the 95% confidence interval for the ensemble mean.

over the northern Asian continent, where mean $\Delta\theta$ is positive in HIST, even though atmospheric moisture content will increase in this region (not shown). This reduction might be related to a drying of the land surface (reduction of available soil moisture) in a warming climate (Seneviratne *et al* 2010). Potentially, this might increase the importance of sensible heating for maintaining blocks over land (Fischer *et al* 2007, Miller *et al* 2021), which warrants further studies.

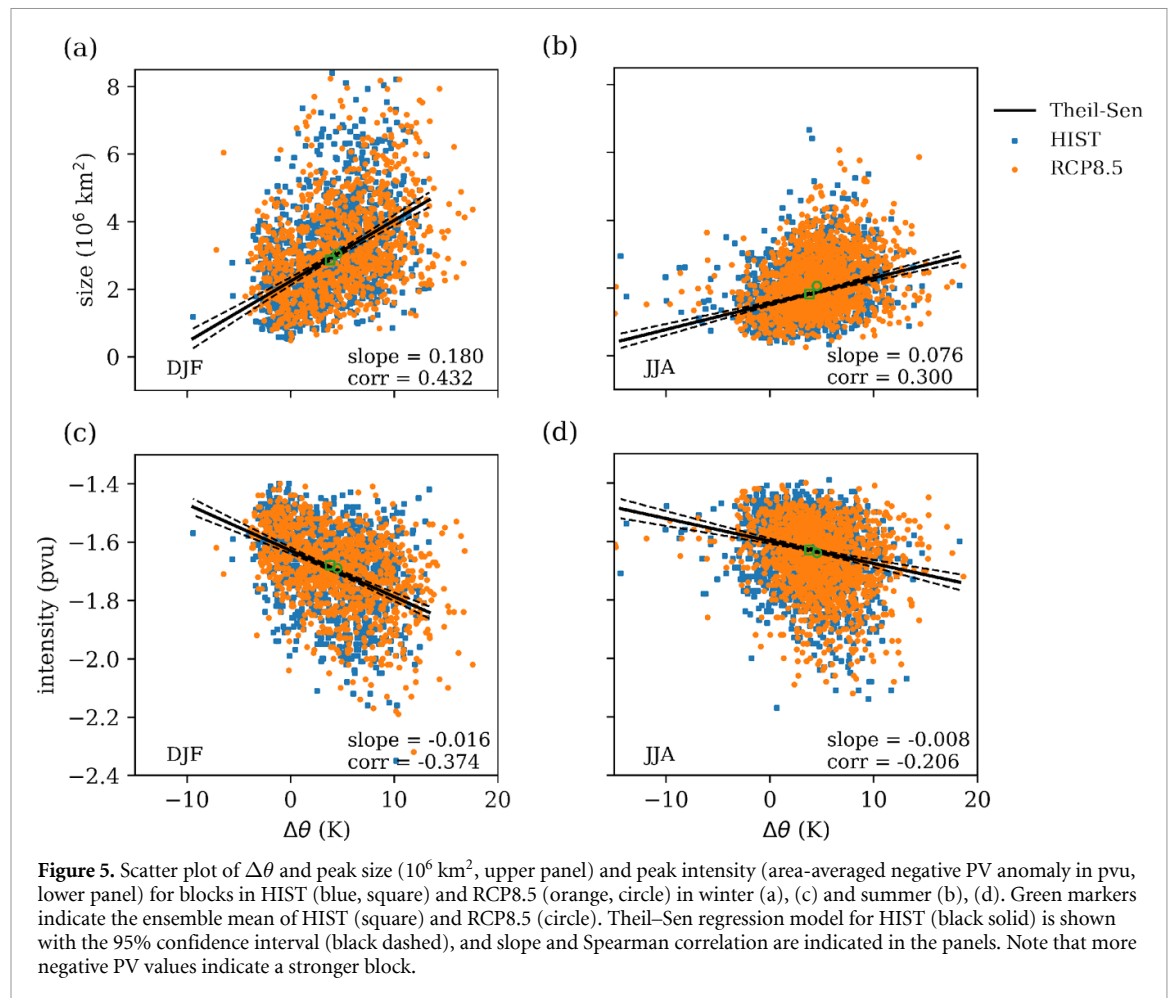
3.4. Response of blocking size and intensity to climate change

The projected changes in the physical processes have the potential to change blocking properties such as intensity, size and duration, which in turn may affect future weather extremes (Nabizadeh *et al* 2021). Here we examine how the intensity and size of blocks respond to increases in $\Delta\theta$, since latent heating typically amplifies blocks (Grams and Archambault 2016, Steinfeld *et al* 2020). We will not discuss blocking duration further as it remains nearly constant in the CESM projections analysed here, which was also observed by Barnes *et al* (2012). To assess potential future changes in intensity and size of blocks, we track individual blocks from onset to decay and show the mean temporal evolution of $\Delta\theta$, intensity and size as a function of blocking age in figure 4.

Figure 4 shows the typically observed lifecycle of blocks (e.g. Dole 1986, Steinfeld and Pfahl 2019), with

a rapid increase in intensity and size during onset, peak intensity and size during the mature phase, and relatively fast decrease in size and intensity until decay. The importance of $\Delta\theta$ varies throughout the lifecycle: latent heating dominates and is strongest during the onset and then gradually declines to an almost negligible contribution (heating and cooling are equally important) when a block decays. The lifecycle averaged over many blocking events is characterized by a gradual evolution. However, individual blocks experience multiple intensification phases and a fluctuation in size, intensity and $\Delta\theta$ during their lifecycle (Lenggenhager *et al* 2019, Steinfeld *et al* 2020).

Figure 4 confirms the general increase in $\Delta\theta$ between HIST and RCP8.5 by about +1 K averaged over the entire blocking lifecycle, with the increase being largest during the onset phase. Blocks are projected to become larger and slightly more intense, with an average increase in peak intensity (strongest negative PV anomaly during the lifecycle) of +0.8% and peak size (largest spatial extent during the lifecycle) of +7%. This increase in intensity and size is stronger in summer (size: +11.9%, intensity: +0.9%) than in winter (size: +5.4%, intensity: +0.63%), although the ensemble agreement is most robust for winter blocks over the ocean basins (not shown), where $\Delta\theta$ increases most. The magnitude of the size increase is consistent with Nabizadeh *et al* (2019),



Tierney *et al* (2021), Bacer *et al* (2022), who used different blocking indices and models. Nabizadeh *et al* (2021) also observed a strengthening of Z500 for winter blocks in CESM-LENS, but small and spatially nonuniform changes for summer blocks.

Given that $\Delta\theta$ and both size and intensity of blocks increase with climate change, one might speculate that increased heating may actually be a driving factor for changes in the size and intensity of future blocking events. Indeed, Steinfeld and Pfahl (2019) observed that moist blocks in ERA-I, defined as blocks with a strong contribution from latent heating, develop faster than dry blocks and are more intense and larger. To test this positive relationship, we fit a non-parametric regression model using the robust Theil–Sen method (Theil 1950, Sen 1968) to see if there is a linear relationship between $\Delta\theta$ (averaged over the blocking lifecycle) and peak intensity or peak size. The Theil–Sen models are fitted separately for winter and summer blocks in CESM-LENS HIST and are shown in figure 5, where each block is a marker. We see that blocks with large $\Delta\theta$ values are larger and more intense, and winter blocks are often larger and more intense than summer blocks, which is also observed in ERA-I (Steinfeld and Pfahl 2019). For winter (figures 5(a) and (c)), the Theil–Sen model estimates a slope of 0.18 ($10^6 \text{ km}^2 \text{ K}^{-1}$) for size and

$-0.016 \text{ (pvu K}^{-1}\text{)}$ for intensity (for each additional 1 K of $\Delta\theta$) with a moderate Spearman correlation of about 0.4. Based on the projected increase in $\Delta\theta$ of +1 K between HIST and RCP8.5, this results in an estimated increase in size of +5.8% and intensity of +0.9%, which agrees well with the projected mean changes between HIST and RCP8.5 (green markers in figure 5 denote the ensemble mean of HIST (square) and RCP8.5 (circle)). In summer (figures 5(b) and (d)), the Theil–Sen model agrees well with the projected changes in intensity (+0.5%), but less well with size, as it estimates weaker increases in size (+4%) than projected by RCP8.5–HIST, but at least the sign of the change is consistent. This difference between winter and summer may be because winter blocks often form over the oceans, where latent heating dominates and projected changes in $\Delta\theta$ are robust, while most summer blocks occur at higher latitudes in the Asian sector, where they form with little contribution from latent heating and projected changes in $\Delta\theta$ are not robust (see again figure 3).

Of course, we acknowledge that figure 5 shows linear correlations, and not necessarily causality between size and intensity on the one hand and $\Delta\theta$ on the other. Recently, however, controlled numerical sensitivity experiments with modified latent heating in the upstream region of the block demonstrated a causal

effect of latent heating on blocking intensity and size (see figure 11 in Steinfeld *et al* 2020). Strong latent heating in rising airstreams and associated diabatic PV reduction and divergent outflow aloft enhance the intensity (negative PV anomaly) and size of blocks in all experiments when compared to their counterparts without latent heating. Furthermore, Nabizadeh *et al* (2021) attributed changes in temperature anomalies under future blocks to enhanced upstream latent heating. Nevertheless, there are other, even competing processes that we have not studied here, but that are known to be important for the occurrence and properties of blocking. These are, most notably, changes in the mean flow and storm tracks due to Arctic amplification and tropical upper-tropospheric warming, and the underlying dynamical processes, which are the subject of ongoing investigations (e.g. Yin 2005, Barnes and Polvani 2013, Harvey *et al* 2014, Peings *et al* 2018). Nabizadeh *et al* (2019) derived a scaling law for the size of blocks, which shows that size scales with the width, strength and latitude of the jet. However, also their scaling law is not able to capture the magnitude of the projected increase in size of summer blocks in CESM-LENS.

4. Conclusion

Weather extremes are often associated with atmospheric blocking (e.g. Schaller *et al* 2018, Kautz *et al* 2022), but how the underlying physical processes in blocking and their relative importance respond to climate change is not yet fully understood (e.g. Woollings *et al* 2018). In this study, we track blocks and apply trajectory analysis to 100 years of present-day and future (~ 2100 , RCP8.5) climate simulations from the CESM large ensemble (CESM-LENS) to identify different physical processes in blocking and quantify how their relative importance changes in a warmer and moisture climate. Consistent with previous studies based on reanalysis data (Pfahl *et al* 2015, Steinfeld and Pfahl 2019), the trajectories reveal two contrasting airstreams: air masses with anomalously low PV are transported into the upper-level block either (a) in ascending airstreams with strong latent heat release (moist processes), or (b) quasi-adiabatically in near-tropopause airstreams along the upper-level jet with weak radiative cooling (dry processes), as illustrated schematically in figure 1. Both moist and dry processes are equally important in present-day climate simulations and are well represented in CESM-LENS when compared against ERA-I reanalysis (Steinfeld and Pfahl 2019), despite the underestimation of blocking activity in CESM-LENS (Davini and D'Andrea 2020).

As known from Steinfeld and Pfahl (2019), the relative importance of moist and dry processes varies regionally and seasonally. The formation and maintenance of blocks over the oceans throughout the year and over the northern Asian continent in summer

are dominated by moist processes (red airstream in figure 1), whereas dry processes dominate in Ural blocks in winter, European blocks in summer, and high-latitude blocks over the Arctic (blue airstream in figure 1).

With a warmer and more humid climate in the future (RCP8.5), moist processes become more important for blocks. Latent heating (+1 K in the median) and the number of strongly ascending WCB airstreams (+15%) increase in winter and summer over large areas of the midlatitudes, but there are pronounced regional and seasonal differences in the changes in physical processes. The increase in latent heating is strongest and most robust in the storm track regions over the oceans, and near-tropopause cooling becomes slightly more important for Ural blocks over land. We further show that the size (+7%) and intensity (+0.8%) of blocks are projected to increase with climate change. Fitting a Theil–Sen regression model, we demonstrate that the changes in the size and intensity of blocks scale well with the increase in latent heating, especially for winter blocks over the oceans. This agrees with previous work that demonstrated the causal effect of latent heating on block intensity and size in numerical case study experiments (Crocì-Maspoli *et al* 2007, Grams and Archambault 2016, Maddison *et al* 2020, Steinfeld *et al* 2020, Neal *et al* 2022).

While consensus on future atmospheric circulation changes in the Northern Hemisphere has not yet been reached (e.g. Shaw *et al* 2016, Woollings *et al* 2018), this study provides further evidence that future changes in blocks are related to moist processes and stronger latent heating (Nabizadeh *et al* 2021). A better understanding of the underlying physical processes in climate models is critically important to improve confidence in climate projections of atmospheric blocking and associated weather extremes.

Data and code availability statement

The blocking identification code CONTRACK (Schwierz *et al* 2004) is available from <https://github.com/steidani/ConTrack> (Steinfeld 2022). The code and information on how to use the Lagrangian analysis tool LAGRANTO (Wernli and Davies 1997, Sprenger and Wernli 2015) can be found from www.lagranto.ethz.ch. ERA-Interim data can be downloaded from the ECMWF web page at: <https://apps.ecmwf.int/datasets/data/interim-full-daily/>.

The data of the CESM-LENS reruns that support the findings of this study are available upon reasonable request from the authors.

Acknowledgments

We thank Heini Wernli (ETH Zürich) for fruitful discussions and input on the manuscript. We are grateful to Erich Fischer (ETH Zürich) and NCAR

for providing the CESM restart files. Daniel Steinfeld acknowledges funding from ETH research Grant ETH-09 15-2.

ORCID iD

Daniel Steinfeld  <https://orcid.org/0000-0001-8525-4904>

References

- Altenhoff A M, Martius O, Croci-Maspoli M, Schwierz C and Davies H C 2008 Linkage of atmospheric blocks and synoptic-scale Rossby waves: a climatological analysis *Tellus A* **60** 1053–63
- Athanasiadis P J, Yeager S, Kwon Y-O, Bellucci A, Smith D W and Tibaldi S 2020 Decadal predictability of North Atlantic blocking and the NAO *npj Clim. Atmos. Sci.* **3** 1–10
- Bacer S, Jomaa F, Beaumet J, Gallée H, Le Bouëdec E, Ménégoz M and Staquet C 2022 Impact of climate change on wintertime European atmospheric blocking *Weather Clim. Dyn.* **3** 377–389
- Barnes E A, Dunn-Sigouin E, Masato G and Woollings T 2014 Exploring recent trends in Northern Hemisphere blocking *Geophys. Res. Lett.* **41** 638–44
- Barnes E A and Polvani L 2013 Response of the midlatitude jets and of their variability, to increased greenhouse gases in the CMIP5 models *J. Clim.* **26** 7117–35
- Barnes E A and Screen J A 2015 The impact of Arctic warming on the midlatitude jet-stream: Can it? Has it? Will it? *WIREs Clim. Change* **6** 277–86
- Barnes E A, Slingo J and Woollings T 2012 A methodology for the comparison of blocking climatologies across indices, models and climate scenarios *Clim. Dyn.* **38** 2467–81
- Berggren R, Bolin B and Rossby C-G 1949 An aerological study of zonal motion, its perturbations and break-down *Tellus* **1** 14–37
- Blackport R and Screen J A 2020 Insignificant effect of Arctic amplification on the amplitude of midlatitude atmospheric waves *Sci. Adv.* **6** eaay2880
- Brunner L, Hegerl G C and Steiner A K 2017 Connecting atmospheric blocking to European temperature extremes in spring *J. Clim.* **30** 585–94
- Brunner L, Schaller N, Anstey J, Sillmann J and Steiner A K 2018 Dependence of present and future European temperature extremes on the location of atmospheric blocking *Geophys. Res. Lett.* **45** 6311–20
- Buehler T, Raible C C and Stocker T F 2011 The relationship of winter season North Atlantic blocking frequencies to extreme cold or dry spells in the ERA-40 *Tellus A* **63** 174–87
- Büeler D and Pfahl S 2019 Potential vorticity diagnostics to quantify effects of latent heating in extratropical cyclones. Part II: application to idealized climate change simulations *J. Atmos. Sci.* **76** 1885–902
- Colucci S J 1985 Explosive cyclogenesis and large-scale circulation changes: implications for atmospheric blocking *J. Atmos. Sci.* **42** 2701–17
- Croci-Maspoli M and Davies H C 2009 Key dynamical features of the 2005/06 European winter *Mon. Weather Rev.* **137** 664–78
- Croci-Maspoli M, Schwierz C and Davies H C 2007 A multifaceted climatology of atmospheric blocking and its recent linear trend *J. Clim.* **20** 633–49
- Davini P and D'Andrea F 2016 Northern Hemisphere atmospheric blocking representation in global climate models: twenty years of improvements? *J. Clim.* **29** 8823–40
- Davini P and D'Andrea F 2020 From CMIP3 to CMIP6: Northern Hemisphere atmospheric blocking simulation in present and future climate *J. Clim.* **33** 10021–38
- Dee D P *et al* 2011 The ERA-interim reanalysis: configuration and performance of the data assimilation system *Q. J. R. Meteorol. Soc.* **137** 553–97
- Deser C, Phillips A, Bourdette V and Teng H 2012 Uncertainty in climate change projections: the role of internal variability *Clim. Dyn.* **38** 527–46
- Dole R M 1986 The life cycles of persistent anomalies and blocking over the North Pacific *Advances in Geophysics (Anomalous Atmospheric Flows and Blocking vol 29)* ed B Saltzman, R Benzi and A C Wiin-Nielsen (Amsterdam: Elsevier) pp 31–69
- Dolores-Tesillos E, Teubler F and Pfahl S 2022 Future changes in North Atlantic winter cyclones in CESM-LE—part 1: cyclone intensity, potential vorticity anomalies and horizontal wind speed *Weather Clim. Dyn.* **3** 429–48
- Drouard M and Woollings T 2018 Contrasting mechanisms of summer blocking over Western Eurasia *Geophys. Res. Lett.* **45** 12040–8
- Drouard M, Woollings T, Sexton D M H and McSweeney C F 2021 Dynamical differences between short and long blocks in the Northern Hemisphere *J. Geophys. Res.: Atmos.* **126** e2020JD034082
- Dunn-Sigouin E and Son S-W 2013 Northern Hemisphere blocking frequency and duration in the CMIP5 models *J. Geophys. Res.: Atmos.* **118** 1179–88
- Fischer E M, Seneviratne S I, Vidale P L, Lüthi D and Schär C 2007 Soil moisture—atmosphere interactions during the 2003 European summer heat wave *J. Clim.* **20** 5081–99
- Grams C M and Archambault H M 2016 The key role of diabatic outflow in amplifying the midlatitude flow: a representative case study of weather systems surrounding western North Pacific extratropical transition *Mon. Weather Rev.* **144** 3847–69
- Harvey B J, Shaffrey L C and Woollings T J 2014 Equator-to-pole temperature differences and the extra-tropical storm track responses of the CMIP5 climate models *Clim. Dyn.* **43** 1171–82
- Harvey B J, Shaffrey L C and Woollings T J 2015 Deconstructing the climate change response of the Northern Hemisphere wintertime storm tracks *Clim. Dyn.* **45** 2847–60
- Hassanzadeh P, Kuang Z and Farrell B F 2014 Responses of midlatitude blocks and wave amplitude to changes in the meridional temperature gradient in an idealized dry GCM *Geophys. Res. Lett.* **41** 5223–32
- Held I M and Soden B J 2006 Robust responses of the hydrological cycle to global warming *J. Clim.* **19** 5686–99
- Hoskins B J, McIntyre M E and Robertson A W 1985 On the use and significance of isentropic potential vorticity maps *Q. J. R. Meteorol. Soc.* **111** 877–946
- Hoskins B and Woollings T 2015 Persistent extratropical regimes and climate extremes *Curr. Clim. Change Rep.* **1** 115–24
- Huguenin M F, Fischer E M, Kotlarski S, Scherrer S C, Schwierz C and Knutti R 2020 Lack of change in the projected frequency and persistence of atmospheric circulation types over Central Europe *Geophys. Res. Lett.* **47** e2019GL086132
- Hurrell J W *et al* 2013 The community earth system model: a framework for collaborative research *Bull. Am. Meteorol. Soc.* **94** 1339–60
- Kautz L-A, Martius O, Pfahl S, Pinto J G, Ramos A M, Sousa P M and Woollings T 2022 Atmospheric blocking and weather extremes over the Euro-Atlantic sector—a review *Weather Clim. Dyn.* **3** 305–36
- Kay J E *et al* 2015 The Community Earth System Model (CESM) large ensemble project: a community resource for studying climate change in the presence of internal climate variability *Bull. Am. Meteorol. Soc.* **96** 1333–49
- Kwon Y-O, Camacho A, Martinez C and Seo H 2018 North Atlantic winter eddy-driven jet and atmospheric blocking variability in the Community Earth System Model version 1 large ensemble simulations *Clim. Dyn.* **51** 3275–89

- Lenggenhager S, Croci-Maspoli M, Brönnimann S and Martius O 2019 On the dynamical coupling between atmospheric blocks and heavy precipitation events: a discussion of the southern Alpine flood in October 2000 *Q. J. R. Meteorol. Soc.* **145** 530–45
- Lenggenhager S and Martius O 2020 Quantifying the link between heavy precipitation and Northern Hemisphere blocking—a Lagrangian analysis *Atmos. Sci. Lett.* **21** e999
- Li M, Woollings T, Hodges K and Masato G 2014 Extratropical cyclones in a warmer, moister climate: a recent Atlantic analogue *Geophys. Res. Lett.* **41** 8594–601
- Luo D, Cha J, Zhong L and Dai A 2014 A nonlinear multiscale interaction model for atmospheric blocking: the eddy-blocking matching mechanism *Q. J. R. Meteorol. Soc.* **140** 1785–808
- Maddison J W, Gray S L, Martínez-Alvarado O and Williams K D 2020 Impact of model upgrades on diabatic processes in extratropical cyclones and downstream forecast evolution *Q. J. R. Meteorol. Soc.* **146** 1322–50
- Madonna E, Wernli H, Joos H and Martius O 2014 Warm conveyor belts in the ERA-interim dataset (1979–2010). Part I: climatology and potential vorticity evolution *J. Clim.* **27** 3–26
- Masato G, Hoskins B J and Woollings T 2013 Winter and summer Northern Hemisphere blocking in CMIP5 models *J. Clim.* **26** 7044–59
- Miller D E and Wang Z 2022 Northern Hemisphere winter blocking: differing onset mechanisms across regions *J. Atmos. Sci.* **79** 1291–309
- Miller D E, Wang Z, Li B, Harnos D S and Ford T 2021 Skillful subseasonal prediction of U. S. extreme warm days and standardized precipitation index in boreal summer *J. Clim.* **34** 5887–98
- Nabizadeh E, Hassanzadeh P, Yang D and Barnes E A 2019 Size of the atmospheric blocking events: scaling law and response to climate change *Geophys. Res. Lett.* **46** 13488–99
- Nabizadeh E, Lubis S W and Hassanzadeh P 2021 The 3D structure of Northern Hemisphere blocking events: climatology, role of moisture and response to climate change *J. Clim.* **34** 9837–60
- Nakamura H, Nakamura M and Anderson J L 1997 The role of high- and low-frequency dynamics in blocking formation *Mon. Weather Rev.* **125** 2074–93
- Nakamura N and Huang C S Y 2018 Atmospheric blocking as a traffic jam in the jet stream *Science* **361** 42–47
- Neal E, Huang C S Y and Nakamura N 2022 The 2021 Pacific Northwest heat wave and associated blocking: meteorology and the role of an upstream cyclone as a diabatic source of wave activity *Geophys. Res. Lett.* **49** e2021GL097699
- O’Gorman P A and Schneider T 2008 Energy of midlatitude transient eddies in idealized simulations of changed climates *J. Clim.* **21** 5797–806
- Peings Y, Cattiaux J, Vavrus S J and Magnusdottir G 2018 Projected squeezing of the wintertime North-Atlantic jet *Environ. Res. Lett.* **13** 074016
- Pfahl S, O’Gorman P A and Singh M S 2015 Extratropical cyclones in idealized simulations of changed climates *J. Clim.* **28** 9373–92
- Pfahl S, Schiwerz C, Croci-Maspoli M, Grams C M and Wernli H 2015 Importance of latent heat release in ascending air streams for atmospheric blocking *Nat. Geosci.* **8** 610–4
- Pfahl S and Wernli H 2012 Quantifying the relevance of atmospheric blocking for co-located temperature extremes in the Northern Hemisphere on (sub-)daily time scales *Geophys. Res. Lett.* **39** L12807
- Rex D F 1950 Blocking action in the middle troposphere and its effect upon regional climate *Tellus* **2** 196–211
- Riboldi J, Lott F, D’Andrea F and Rivière G 2020 On the linkage between Rossby wave phase speed, atmospheric blocking and arctic amplification *Geophys. Res. Lett.* **47** e2020GL087796
- Schaller N, Sillmann J, Anstey J, Fischer E M, Grams C M and Russo S 2018 Influence of blocking on Northern European and Western Russian heatwaves in large climate model ensembles *Environ. Res. Lett.* **13** 054015
- Schiemann R, Athanasiadis P, Barriopedro D, Doblas-Reyes F, Lohmann K, Roberts M J, Sein D V, Roberts C D, Terray L and Vidale P L 2020 Northern Hemisphere blocking simulation in current climate models: evaluating progress from the Climate Model Intercomparison Project Phase 5 to 6 and sensitivity to resolution *Weather Clim. Dyn.* **1** 277–92
- Schneider T, O’Gorman P A and Levine X J 2010 Water vapor and the dynamics of climate changes *Rev. Geophys.* **48** RG3001
- Schiwerz C, Croci-Maspoli M and Davies H C 2004 Perspicacious indicators of atmospheric blocking *Geophys. Res. Lett.* **31** L06125
- Sen P K 1968 Estimates of the regression coefficient based on Kendall’s tau *J. Am. Stat. Assoc.* **63** 1379–89
- Seneviratne S I, Corti T, Davin E L, Hirschi M, Jaeger E B, Lehner I, Orlowsky B and Teuling A J 2010 Investigating soil moisture–climate interactions in a changing climate: a review *Earth-Sci. Rev.* **99** 125–61
- Serreze M C and Barry R G 2011 Processes and impacts of Arctic amplification: a research synthesis *Glob. Planet. Change* **77** 85–96
- Shaw T A et al 2016 Storm track processes and the opposing influences of climate change *Nat. Geosci.* **9** 656–64
- Shutts G J 1983 The propagation of eddies in diffluent jetstreams: eddy vorticity forcing of ‘blocking’ flow fields *Q. J. R. Meteorol. Soc.* **109** 737–61
- Sillmann J and Croci-Maspoli M 2009 Present and future atmospheric blocking and its impact on European mean and extreme climate *Geophys. Res. Lett.* **36** L10702
- Sillmann J, Croci-Maspoli M, Kallache M and Katz R W 2011 Extreme cold winter temperatures in Europe under the influence of North Atlantic atmospheric blocking *J. Clim.* **24** 5899–913
- Sprenger M and Wernli H 2015 The LAGRANTO Lagrangian analysis tool—version 2.0 *Geosci. Model Dev.* **8** 2569–86
- Steinfeld D 2022 ConTrack—contour tracking (available at: <https://github.com/steidani/ConTrack>)
- Steinfeld D, Boettcher M, Forbes R and Pfahl S 2020 The sensitivity of atmospheric blocking to upstream latent heating—numerical experiments *Weather Clim. Dyn.* **1** 405–26
- Steinfeld D and Pfahl S 2019 The role of latent heating in atmospheric blocking dynamics: a global climatology *Clim. Dyn.* **53** 6159–80
- Tamarin T and Kaspi Y 2016 The poleward motion of extratropical cyclones from a potential vorticity tendency analysis *J. Atmos. Sci.* **73** 1687–707
- Theil H 1950 A rank-invariant method of linear and polynomial regression analysis. I, II, III *Ned. Akad. Wet. Proc. A* **53** 386–92, 521–5, 1397–412
- Tierney G, Robinson W A, Lackmann G and Miller R 2021 The sensitivity of persistent geopotential anomalies to the climate of a moist channel model *J. Clim.* **34** 5093–108
- Trenberth K E 1999 Conceptual framework for changes of extremes of the hydrological cycle with climate change *Clim. Change* **42** 327–39
- Wehrli K, Guillod B P, Hauser M, Leclair M and Seneviratne S I 2019 Identifying key driving processes of major recent heat waves *J. Geophys. Res.: Atmos.* **124** 11746–65
- Wernli H and Davies H C 1997 A Lagrangian-based analysis of extratropical cyclones. I: the method and some applications *Q. J. R. Meteorol. Soc.* **123** 467–89

- Woollings T, Barriopedro D, Methven J, Son S-W, Martius O, Harvey B, Sillmann J, Lupo A R and Seneviratne S 2018 Blocking and its response to climate change *Curr. Clim. Change Rep.* **4** 287–300
- Yamazaki A and Itoh H 2013 Vortex–vortex interactions for the maintenance of blocking. Part I: the selective absorption mechanism and a case study *J. Atmos. Sci.* **70** 725–42
- Yettella V and Kay J E 2017 How will precipitation change in extratropical cyclones as the planet warms? Insights from a large initial condition climate model ensemble *Clim. Dyn.* **49** 1765–81
- Yin J H 2005 A consistent poleward shift of the storm tracks in simulations of 21st century climate *Geophys. Res. Lett.* **32** L18701